J|A|C|S
ARTICLES
Published on Web 01/31/2004

# Nature of One-Dimensional Short Hydrogen Bonding: Bond Distances, Bond Energies, and Solvent Effects

Seung Bum Suh, Jong Chan Kim, Young Cheol Choi, Sunggoo Yun, and Kwang S. Kim*

*Contribution from the National Creative Research Initiative Center for Superfunctional Materials, Department of Chemistry, Division of Molecular and Life Sciences, Pohang University of Science and Technology, San 31, Hyojadong, Namgu, Pohang 790-784, Korea*

Received July 29, 2003; E-mail: kim@postech.ac.kr

***Abstract:*** On the basis of recently synthesized calix[4]hydroquinone (CHQ) nanotubes which were self-assembled with infinitely long one-dimensional (1-D) short hydrogen bonds (SHB), we have investigated the nature of 1-D SHB using first-principles calculations for all the systems including the solvent water. The H-bonds relay (i.e., contiguous H-bonds) effect in CHQs shortens the H···O bond distances significantly (by more than 0.2 Å) and increases the bond dissociation energy to a large extent (by more than ∼4 kcal/mol) due to the highly enhanced polarization effect along the H-bond relay chain. The H-bonds relay effect shows a large increase in the chemical shift associated with the SHB. The average binding energies for the infinite 1-D H-bond arrays of dioles and dions increase by ∼4 and ∼9 kcal/mol per H-bond, respectively. The solvent effect (due to nonbridging water molecules) has been studied by explicitly adding water molecules in the CHQ tube crystals. This effect is found to be small with slight weakening of the SHB strength; the H···O bond distance increases only by 0.02 Å, and the average binding energy decreases by ∼1 kcal/mol per H-bond. All these results based on the first-principles calculations are the first detailed analysis of energy gain by SHB and energy loss by solvent effect, based on a partitioning scheme of the interaction energy components. These reliable results elucidate not only the self-assembly phenomena based on the H-bond relay but also the solvent effect on the SHB strength.

## I. Introduction

It is well-known that nature utilizes the self-assembly process for many interesting chemical and biomolecular systems as well as proteins and nucleic acids foldings.[1] The advantage of the self-assembly process is the ability to self-correct the process, resulting in an error-free process along with high yields which can be utilized to the nanomaterial synthetic process. Thus, it is very important to understand the major components leading to the self-assembly process including the self-synthesis process, which would ultimately be useful to design new functional materials and nanomaterials. Indeed, based on understanding the molecular interactions governing the self-assembly process, we have recently synthesized calix[4]hydroquinone (CHQ) nanotubes self-assembled with infinitely long one-dimensional (1-D) short hydrogen bonds (SHB) (Figure 1).[2] In this case, the H-bond length is particularly short (∼2.65 Å) compared with the normal H-bond length (2.8−2.9 Å). Therefore, it is very important to understand the increased binding strength of 1-D SHB in comparison with the normal H-bond.

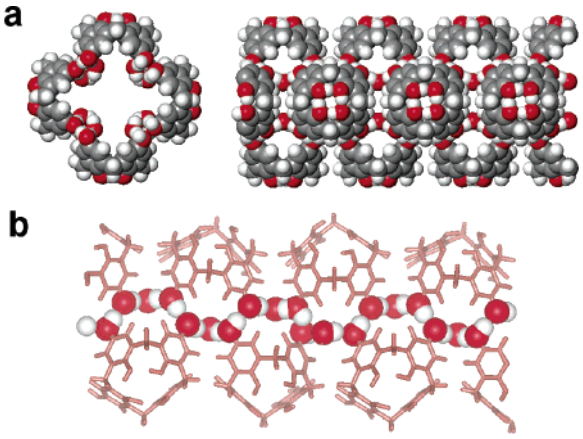


***Figure 1.*** Longitudinal H-bond relay comprised of CHQs and water. (a) Tubular polymer structure of a single nanotube obtained with X-ray analysis for the heavy atoms and with ab initio calculations for the H orientations (top and side views). (b) One of four pillar frames of short H-bonds (shown as the space-filled part with O atoms in red and H atoms in white) represents a 1-D H-bond relay composed of a series of consecutive OH groups [hydroxyl groups (−OH) in CHQs and the OHs in water molecules].

As H-bonding has been one of the most important interaction forces in molecular assembly, it is natural to find the studies

(1) (a) Steed, J. W., Atwood, J. L., Eds. *Supramolecular Chemistry*; John Wiley & Sons: West Sussex, UK, 2000. (b) Atwood, J. L., Davis, J. E. D., MacNicol, D. D., Vögtle, F., Lehn, J.-M., Eds. *Comprehensive Supramolecular Chemistry*; Elsevier: Amsterdam, 1996; Vols. 1−11.

(2) (a) Hong, B. H.; Lee, J. Y.; Lee, C.-W.; Kim, J. C.; Bae, S. C.; Kim, K. S. *J. Am. Chem. Soc.* **2001**, *123*, 10748−10749. (b) Hong, B. H.; Bae, S. C.; Lee, C.-W.; Jeong, S.; Kim, K. S. *Science* **2001**, *294*, 348−351. (c) Kim, K. S. *Curr. Appl. Phys.* **2002**, *2*, 65−69. (d) Kim, K. S. *Bull. Korean Chem. Soc.* **2003**, *24*, 757−762. (e) Kim, K. S.; Suh, S. B.; Kim, J. C.; Hong, B. H.; Lee, E. C.; Yun, S.; Tarakeshwar, P.; Lee, J. Y.; Kim, Y.; Ihm, H.; Kim, H. G.; Lee, J. W.; Kim, J. K.; Lee, H. M.; Kim, D.; Cui, C.; Youn, S. J.; Chung, H. Y.; Choi, H. S.; Lee, C.-W.; Cho, S. J.; Jeong, S.; Cho, J.-H. *J. Am. Chem. Soc.* **2002**, *124*, 14268−14279.


**10.1021/ja037607a CCC: $27.50** 

on such molecular systems involving H-bonds.[3] One of the earliest and most simple of such studies is of the self-assembled water clusters.[4] In addition, there have been many other studies such as aqueous clusters, alcohol clusters, and hydrogen halide clusters.[5] In the H-bonded molecular clusters in the forms of chains, cycles, and other networks, the H-bonds are strengthened by the polarization effect.[6] In particular, Hermansson and co-workers[7] have investigated the polarization effect of water chains. According to Salahub and co-workers,[8] this polarization effect is large in isolated linear polypeptides. This effect was further stressed by Wu and co-workers.[9] There have been a number of studies on the H-bond relay effect.[10] In particular, Dannenberg and co-workers[11] have investigated the H-bond strength of linear structures of 1,3-propanedione,[12] which is very useful to help understand the strong H-bond.

The short H-bond, the length of which is less than 2.6 Å, has often been found in the cases where an OH (or NH) bond involves H-bonding with an adjacent oxyanion in enzymes.[13] Since this type of H-bond has often been considered to play an important role in enzyme mechanisms, it has been termed as low-barrier H-bond (LBHB), or more generally as short strong H-bond (SSHB).[14,15] On the other hand, it should be also mentioned that another scientific group tends to underscore the role of SSHB in enzymes, and instead stresses the role preorganization (associated with the polarized structure of enzymes in favor of the transition states).[16] Nevertheless, as the magnitude of the binding energy is not yet clearly understood, the issues of H-bonding strength and the role of SSHB are still controversial.[15,16]

While the issue of SSHB is often related to the enzymes with anionic sites, the CHQ nanotubes do not involve such sites. It is thus interesting to note that these neutral systems have SHBs which are almost comparable in bond length to SSHBs. In particular, since the 1-D H-bond arrays in CHQ nanotubes are built up with only OH groups, this consecutive H-bond relay is contrasted to other 1-D linear H-bond chains such as polydiols and polydiones. This 1-D consecutive H-bond array should be very interesting in that it would be similar to the 1-D linear network of water in membrane channels or in carbon nanotubes.[7,17] Therefore, elucidation of the origin of these 1-D H-bonds and their strength would be of importance, and it would help understand the molecular assembly processes. This elucidation would also be useful to find the correlation and difference between the SHB involving neutral (but partially ionic) systems and SSHB involving ionic systems. Here, we elucidate how the H-relay effect due to additional H-bonds by the hydroquinone moieties ($Q_h$) and the bridging water molecules ($W_b$) shortens the H···O bond distance and increases its binding energy in the infinitely long 1-D SHBs of CHQ nanotubes, and we compare this 1-D consecutive H-bond relay with other 1-D H-bond relays.

## II. Theoretical Methods

To obtain the H-bond distances in an 1-D H-bond relay, we have carried out density functional calculations employing Becke's three parameters using Lee−Yang−Parr functionals (B3LYP) with the 6-31G* basis set. For comparison, Moller−Plesset second-order perturbation (MP2) calculations were also performed for the dimer systems. The B3LYP/6-31G* and MP2/6-31G* calculations were carried out using a Gaussian suite of programs.[18] The basis set superposition error (BSSE) correction has been made, and these technical details and the associated problems have been discussed in many previous works.[19] It is not feasible yet to do MP2 calculations to investigate the effect of a long H-bond relay; thus, we carried out B3LYP calculations. Furthermore, the infinitely long H-bond relay effect in the CHQ crystal can be investigated at the present status only at the level of plane wave density functional theory (PW-DFT) using


(3) (a) Scheiner, S. *Hydrogen Bonding*; Oxford University Press: New York, 1997. (b) Jeffrey, G. A. *An Introduction to Hydrogen Bond*; Oxford University Press: New York, 1997. (c) Scheiner, S.; Kar, T.; Pattanayak, J. *J. Am. Chem. Soc.* **2002**, *124*, 13257−13264.

(4) Kim, K. S.; Dupuis, M.; Lie, G. C.; Clementi, E. *Chem. Phys. Lett.* **1986**, *131*, 451−456.

(5) (a) Sum, A. K.; Sandler, S. *J. Phys. Chem.* **2000**, *104*, 1121−1129. (b) Reimann, B.; Buchhold, K.; Barth, H.-D.; Brutschy, B.; Tarakeshwar, P.; Kim, K. S. *J. Chem. Phys.* **2002**, *117*, 8805−8822. (c) Masella, M.; Flament, J. P. *J. Chem. Phys.* **1998**, *108*, 7141−7151. (d) Lee, H. M.; Kim, D.; Kim, K. S. *J. Chem. Phys.* **2002**, *116*, 5509−5520. (e) Kim, K. S.; Lee, J. Y.; Choi, H. S.; Kim, J.; Jang, J. H. *Chem. Phys. Lett.* **1997**, *265*, 497−502. (f) Tarakeshwar, P.; Choi, H. S.; Kim, K. S. *J. Am. Chem. Soc.* **2001**, *123*, 3323−3331. (g) Lee, H. M.; Lee, S.; Kim, K. S. *J. Chem. Phys.* **2003**, *119*, 187−194. (h) Manojkumar, T. K.; Choi, H. S.; Tarakeshwar, P.; Kim, K. S. *J. Chem. Phys.* **2003**, *118*, 8681−8686.

(6) Lee, H. M.; Suh, S. B.; Lee, J. Y.; Tarakeshwar, P.; Kim, K. S. *J. Chem. Phys.* **2000**, *112*, 9759−9772; **2001**, *114*, 3343.

(7) Hermansson, K.; Alfredsson, M. *J. Chem. Phys.* **1999**, *111*, 1993−2000.

(8) (a) Guo, H.; Salahub, D. R. *J. Angew. Chemie, Int, Ed.* **1998**, *37*, 2985−2990. (b) Guo, H.; Gresh, N.; Roques, B. P.; Salahub, D. R. *J. Phys. Chem. B* **2000**, *104*, 9746−9754.

(9) (a) Zhao, Y.-L.; Wu, Y.-D. *J. Am. Chem. Soc.* **2002**, *124*, 1570−1571. (b) Wu, Y.-D.; Zhao, Y.-L. *J. Am. Chem. Soc.* **2001**, *123*, 5313−5319.

(10) (a) Guedes, R. C.; Couto, P. C.; Carbral, B. J. C. *J. Chem. Phys.* **2003**, *118*, 1272−1281. (b) Rincon, L.; Almeida, R.; Garcia-Aldea, D.; Riega, H. D. *J. Chem. Phys.* **2001**, *114*, 5552−5561. (c) Tsuzuki, S.; Houjou, B.; Nagawa, Y.; Goto, M.; Hiratani, K. *J. Am. Chem. Soc.* **2001**, *123*, 4255−4258.

(11) (a) Kobko, N.; Paraskevas, L.; del Rio, E.; Dannenberg, J. J. *J. Am. Chem. Soc.* **2001**, *123*, 4348−4349. (b) Dannenberg, J. J.; Haskamp, L.; Masaunov, A. *J. Phys. Chem. A* **1999**, *103*, 7083−7086. (c) Masunov, A.; Dannenberg, J. J. *J. Phys. Chem. B* **2000**, *104*, 806−810. (d) Simon, S.; Duran, M.; Dannenberg, J. J. *J. Phys. Chem. A* **1999**, *103*, 1640−1643.

(12) Etter, M. C.; Urbanczyk-Lipkowska, Z.; Jahn, D. A.; Frye, J. *J. Am. Chem. Soc.* **1986**, *108*, 5871−5876.

(13) (a) Kim, K. S.; Kim, D.; Lee, J. Y.; Tarakeshwar, P.; Oh, K. S. *Biochemistry* **2002**, *41*, 5300−5306. (b) Cho, H.−S.; Ha, N.−C.; Choi, G.; Kim, H.−J.; Lee, D.; Oh, K. S.; Kim; K. S.; Lee, W.; Choi, K. Y.; Oh, B.−H. *J. Biol. Chem.* **1999**, *274*, 32863−32868. (c) Oh, K. S.; Cha, S.-S.; Kim, D.-H.; Cho, H.-S.; Ha, N.-C.; Choi, G.; Lee, J. Y.; Tarakeshwar, P.; Son, H. S.; Choi, K. Y.; Oh, B. H.; Kim, K. S. *Biochemistry* **2000**, *39*, 13891−13896. (d) Kim, K. S.; Oh, K. S.; Lee, J. Y. *Proc. Natl. Acad. Sci. U*.S.A. **2000**, *97*, 6373−6378.

(14) (a) Cleland, W. W.; Kreevoy, M. M. *Science* **1994**, *264*, 1887−1890. (b) Frey, P. A.; Whitt, S. A.; Tobin, J. B. *Science* **1994**, *264*, 1927−1930. (c) Gerlt, J. A.; Grassman, P. G. *J. Am. Chem. Soc.* **1993**, *115*, 11552−11568. (d) Zhao, Q.; Abeygunawardana, C.; Talalay, P.; Mildvan, A. S. *Proc. Natl. Acad. Sci. U.S.A.* **1996**, *93*, 8220−8224. (e) Perrin, C. L.; Nielson, J. B. *Annu. Rev. Phys. Chem.* **1997**, *48*, 511−544. (g) Stryer, L. *Biochemistry*, 4ed.; Seoul Printing: Seoul, 1995.

(15) (a) Cleland, W. W.; Kreevoy, M. M. *Science* **1995**, *269*, 104−104. (b) Frey, P. A. *Science* **1995**, *269*, 104−106. (b) Lin, J.; Westler, W. M.; Cleland, W. W.; Markely, J. L.; Frey, P. A. *Proc. Natl. Acad. Sci. U.S.A.* **1998**, *95*, 14664−14668. (c) Cleland, W. W.; Frey, P. A.; Gerlt, J. A. *J. Biol. Chem.* **1998**, *273*, 25529−25532. (d) Lin, J.; Frey, P. A. *J. Am. Chem. Soc.* **2000**, *122*, 11258−11259. (e) Neidhart, D.; Wei, Y.; Cassidy, C.; Lin, J.; Cleland, W. W.; Frey, P. A. *Biochemistry* **2001**, *40*, 2439−2447. (f) Shan, S.; Loh, S.; Herschlag, D. *Science* **1996**, *272*, 97−101. (g) Kollman, P. A.; Kuhn, B.; Donini, O.; Perakyla, M.; Stanton, R.; Bakowies, D. *Acc. Chem. Res.* **2001**, *34*, 72−79.

(16) (a) Warshell, A.; Parazyan, A. *Proc. Natl. Acad. Sci. U.S.A.* **1996**, *93*, 13665−13670. (b) Åqvist, J.; Kolmodin, K.; Florian, J.; Warshel, A. *Chem. Biol.* **1999**, *6*, 71−80.

(17) (a) Mei, H. S.; Tuckerman, M. E.; Sagnella, D. E.; Klein, M. L. *J. Phys.* Chem. **1998**, *102*, 10446−10458. (b) Kim, K. S.; Nguyen, H. L.; Swaminathan, P. K.; Clementi, E. *J. Phys.* Chem. **1985**, *89*, 2870−2876. (c) Kim, K. S. *J. Comput.* Chem. **1985**, *6*, 256−263.

(18) Frisch, M. J.; Trucks, G. W.; Schlegel, H. B.; Scuseria, G. E.; Robb, M. A.; Cheeseman, J. R.; Zakrzewski, V. G.; Montgomery, J. A., Jr.; Stratmann, R. E.; Burant, J. C.; Dapprich, S.; Millam, J. M.; Daniels, A. D.; Kudin, K. N.; Strain, M. C.; Farkas, O.; Tomasi, J.; Barone, V.; Cossi, M.; Cammi, R.; Mennucci, B.; Pomelli, C.; Adamo, C.; Clifford, S.; Ochterski, J.; Petersson, G. A.; Ayala, P. Y.; Cui, Q.; Morokuma, K.; Malick, D. K.; Rabuck, A. D.; Raghavachari, K.; Foresman, J. B.; Cioslowski, J.; Ortiz, J. V.; Stefanov, B. B.; Liu, G.; Liashenko, A.; Piskorz, P.; Komaromi, I.; Gomperts, R.; Martin, R. L.; Fox, D. J.; Keith, T.; Al-Laham, M. A.; Peng, C. Y.; Nanayakkara, A.; Gonzalez, C.; Challacombe, M.; Gill, P. M. W.; Johnson, B. G.; Chen, W.; Wong, M. W.; Andres, J. L.; Head-Gordon, M.; Replogle, E. S.; Pople, J. A. *Gaussian 98*; Gaussian, Inc.: Pittsburgh, 1999.

pseudopotentials. This calculation also requires extensive computing time. For the PW-DFT method, a generalized gradient approximation (GGA) of Perdew and Wang[20] and the Vanderbilt pseudopotentials[21] were employed, as in our previous works on condensed matter systems.[22] To deal with a very large system, we used a Vienna ab initio simulation package (VASP) of programs.[23] The unit cell for the periodic box was set to that of the X-ray crystal data ($25.03 \times 23.30 \times 11.63$ Å$^3$) in which a half unit cell corresponding to a single nanotube has 4 CHQs with 8 bridging water molecules and the other half unit cell has the copy of the first one by symmetry operation. The cutoff energy of the plane wave basis set is 20 Ry. It should be noted that PW-DFT is free from BSSE, because plane wave basis sets cover the whole space almost uniformly unlike the Gaussian orbitals spanning only a local region.

We also investigated the solvent effect by explicitly adding water molecules in the CHQ tube after calculating the solvent accessible volume.[24,25] We found that the appropriate number of water molecules to be accommodated in a half unit cell is 24. The initial configuration of water molecules in the CHQ tube was randomized by the annealing technique using Monte Carlo simulations.[3,25] Then, the system was slowly quenched by molecular dynamics simulations, followed by room-temperature molecular dynamics simulations for 10 ps, while the main building frame of the molecular system was fixed to the PW-DFT optimized structure which is very close to the X-ray structure. In these classical Monte Carlo and molecular dynamics simulations, the optimized potential for liquid simulations (OPLS)[26] was employed, while the structure of the CHQ tube was kept under restraint. After this equilibration, to obtain one of the most significant structures of the whole system comprising CHQs and bridging water molecules in the absence/presence of solvent water molecules, we optimized the geometry of the whole system (comprising up to 176 C/O atoms and 160 H atoms in a half unit cell in the presence of solvent water molecules and their copy for the other half unit cell by symmetry operation) using plane wave pseudopotential methods in the periodic boundary condition of the X-ray crystal unit cell. This calculation would be considered to be one of the largest systems performed using PW-DFT methods. In this way, the solvent effect in the explicit presence of water molecules was analyzed with a new approach to use a partitioning scheme of interaction energy components.

Chemical shifts of the H atom involving the H-bonds were investigated with the gauge-independent atomic orbital (GIAO) method using the Hartree−Fock (HF)/6-31G* calculations at the B3LYP/6-31G* and PW-DFT optimized geometries.

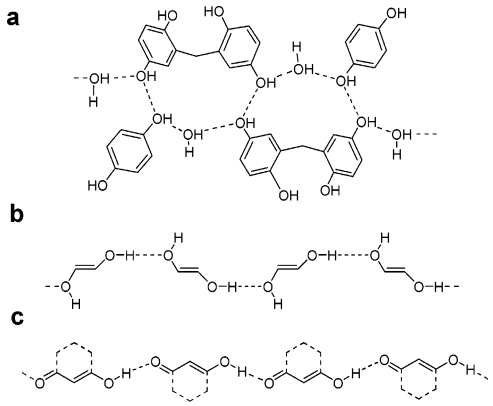


***Figure 2.*** Schematic of 1-D H-bonds systems. (a) CHQ nanotube fragment with nine consecutive H−Bonds. (b) 1-D H-bond system of poly 1,2 ethanedioles (diols). (c) 1-D H-bond system of poly 1,3 propanedione (diones).

## III. Results and Discussion

**III. A. Normal H-Bonds in the Dimer Formation.** To understand the SHB due to the H-relay, we have investigated the 1-D H-bond relay systems of a CHQ nanotube, a linear chain of diols, and a linear chain of diones (Figure 2). In the case of the CHQ nanotube, they are involved in three types of H-bonds represented as $W_b>Q_h$, $Q_h>Q_h$, and $Q_h>W_b$ (Figure 3a−c), where the interactions between a proton-donor (D) and a proton acceptor (A) will be denoted as D>A (where ">" represents the −OH bond orientation), and $W_b$ denotes a bridging water molecule. The B3LYP/6-31G* H-bonding energies with 50% BSSE correction[18a] of the three cases, $W_b>Q_h$, $Q_h>Q_h$, and $Q_h>W_b$, are 5.4, 6.3, and 8.6 kcal/mol, respectively (Table 1). These are in reasonable agreement with the corresponding PW-DFT values (5.6, 4.6, and 8.4 kcal/mol). The B3LYP/6-31G* binding energies are also similar to the MP2/6-31G* values (5.6, 7.8, and 8.5 kcal/mol). In the case of MP2/6-31G* calculations for $Q_h>Q_h$, the $\pi-\pi$ interaction between two $Q_h$'s which is not obtainable in the DFT calculation is included in the binding energy. Thus, excluding the $\pi-\pi$ interaction (1.4 kcal/mol which was obtained from the MP2 calculation of the system wherein the two OH's involving H-bond are replaced by two H's), the MP2 pure H-bond energy for $Q_h>Q_h$ is 6.4 kcal/mol, in good agreement with the DFT result. Although the pure H-bond energies of $Q_h>Q_h$ at the MP2 and B3LYP levels are somewhat larger than that of PW-DFT level, the H-bond distance between the neighbored $Q_h$'s is almost same regardless of the levels of theory, because the H-bond for the $Q_h>Q_h$ is present between two $Q_h$ moieties in the well-defined bell-shaped CHQ monomer structure composed of four $Q_h$ moieties linked by the methyl groups. Thus, the $Q_h>Q_h$ interaction energy does not affect the H-bond relay structure regardless of the levels of theory.

The MP2/6-31G* H-bond distances (O···H) in $W_b>Q_h$, $Q_h>Q_h$, and $Q_h>W_b$ are 2.01, 1.91, and 1.87 Å, respectively. These are similar to the B3LYP/6-31G* values (1.99, 1.90, and 1.83 Å) and the PW-DFT values (1.97, 1.88, and 1.81 Å) (Table 1). It is interesting to note the differences in H-bond distance and H-bond energy between $W_b>Q_h$ and $Q_h>W_b$. In the case of $Q_h>W_b$, the values of ($q_H$,$q_O$), which are the natural bond

(19) (a) Kim, K. S.; Tarakeshwar, P.; Lee, J. Y. *Chem. Rev.* **2000**, *100*, 4145−4186. (b) Davidson, E. R.; Chakravorty, S. J. *Chem. Phys. Lett.* **1994**, *217*, 48−54. (c) Loushin, S. K.; Liu, S.; Dykstra, C. E. *J. Chem. Phys.* **1986**, *97*, 2720−2725. (d) Kim, J.; Kim, K. S. *J. Chem. Phys.* **1998**, *100*, 5886−5895. (e) Kim, K. S.; Mhin, B. J.; Choi, U.-S.; Lee, K. *J. Chem. Phys.* **1992**, *97*, 6649−6662. (f) Marsden, C. J.; Smith, G. J.; Pople, J. A.; Schaefer, H. F.; Radom, L. *J. Chem. Phys.* **1991**, *91*, 1825−1828. (g) Tschumper, G. S.; Leininger, M. L.; Hoffman, B. C.; Valeev, E. F.; Schaefer, H. F.; Quack, M. *J. Chem. Phys.* **2002**, *116*, 690−700.
(20) (a) Wang, Y.; Perdew, J. P. *Phys. Rev. B* **1991**, *43*, 8911−8916. (b) Perdew, J. P.; Wang, Y. *Phys. Rev. B* **1992**, *45*, 13244−13249.
(21) Vanderbilt, D. *Phys. Rev. B* **1990**, *41*, 7892−7895.
(22) (a) Suh, S. B.; Hong, B. H.; Tarakeshwar, P.; Youn, S. J.; Jeong, S.; Kim, K. S. *Phys. Rev. B* **2003**, *67*, 241402(R). (b) Geng, W.-T.; Kim, K. S. *Phys. Rev. B* **2003**, *67*, 233403. (c) Cho, J.-H.; Kim, K. S. *Phys. Rev. B* **2000**, *62*, 1607−1610. (e) Cho, J.-H.; Park, J. M.; Kim, K. S. *Phys. Rev. B* **2000**, *62*, 9981−9984. (f) Cho, J. H.; Kleinman, L.; Jin, K.-J.; Kim, K. S. *Phys. Rev. B* **2002**, *66*, 113306. (g) Nautiyal, T.; Youn, S. J.; Kim, K. S. *Phys. Rev. B* **2003**, *68*, 033407.
(23) (a) Kresse, G.; Furthmuller, J. *VASP the Guide*; Vienna, 2001. (b) Kresse, G.; Furthmuller, J. *Phys. Rev. B* **1996**, *54*, 11169−11186. (c) Kresse, G.; Hafner, J. *J. Phys. Rev. B* **1993**, *47*, R558.
(24) The unit cell is divided into equal size of boxes [$125 \times 117 \times 58$ cells with the volume of ($\sim$0.2 Å)$^3$]. If the center of each box is within the van der Waals contact distance from the CHQ heavy atoms, the volume of that box is excluded from the solvent accessible volume.
(25) (a) Kim, K. S.; Corongiu, G.; Clementi, E. *J. Biomol. Struct. Dynamics* **1983**, *1*, 263−285. (b) Kim, K. S.; Clementi, E. *J. Am. Chem. Soc.* **1985**, *107*, 227−234. (c) Kim, K. S.; Clementi, E. *J. Am. Chem. Soc.* **1985**, *107*, 5504−5513.
(26) Jorgensen, W. L.; Severance, D. L. *J. Am. Chem. Soc.* **1990**, *112*, 4768−4774.

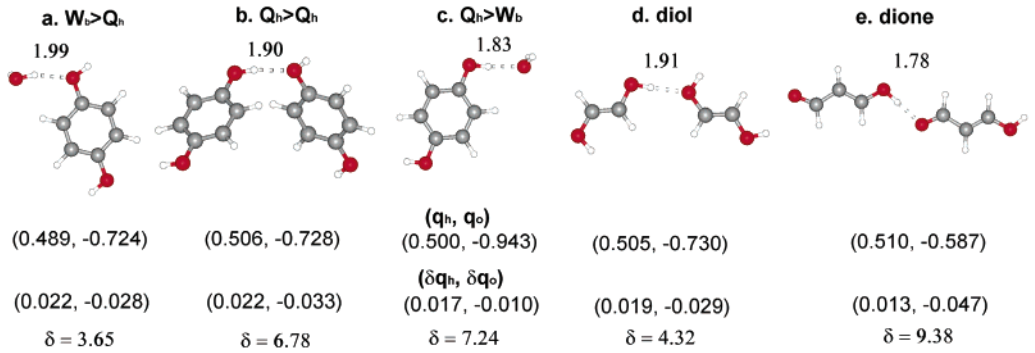


***Figure 3.*** Three types of H-bonding involved with 1-D H-bonds of CHQ nanotubes [(a) $W_b>Q_h$, (b) $Q_h>Q_h$, and (c) $Q_h>W_b$] and the H-bonds in (d) the diol dimer and (e) the dione dimer. The H···O bond distances (Å), atomic charges ($q_H$ and $q_O$ in au) and their changes with respect to the values of the isolated systems ($\Delta q_H$ and $\Delta q_O$ in au), and proton chemical shifts ($\delta$ in ppm) are given at the B3LYP/6-31G* level.

***Table 1.*** Interaction Energies (kcal/mol) and O···O and O···H Distances (in Å in parentheses) for the Three H-Bonding Types (without consideration of the H-bond relay effect) of the CHQ Nanotube and the H-Bonds of the Diol Dimer and the Dione Dimer[a]

| | $W>Q_h$ | $Q_h>Q_h$ | $Q_h>W$ | diol | dione |
|---|---|---|---|---|---|
| MP2/6-31G* | −5.61±1.80 | −7.82±2.05 | −8.45±1.29 | −6.33±0.89 | −11.24±1.35 |
| | (2.94, 2.01) | (2.87, 1.91) | (2.85, 1.87) | (2.88, 1.91) | (2.77, 1.78) |
| B3LYP/6-31G* | −5.38±1.67 | −6.30±1.44 | −8.59±1.21 | −5.87±0.72 | −12.29±1.08 |
| | (2.92, 1.99) | (2.86, 1.90) | (2.81, 1.83) | (2.86, 1.89) | (2.71, 1.72) |
| PW-DFT | −5.6 | −4.6 | −8.4 | | |
| | (2.97, 1.97) | (2.88, 1.88) | (2.82, 1.81) | | |

[a] The PW-DFT method is free from BSSE. All other interaction energies are given as a median value between BSSE-uncorrected and BSSE-corrected values with the error bar of 50%-BSSE (the lower and upper bounds are the BSSE-uncorrected and BSSE-corrected values, respectively).

***Table 2.*** H-Bond Interaction Energies (kcal/mol) and H···O Distances (Å in parentheses) in H-Bond Relay Systems at the B3LYP/6-31G* Level[a]

| type: D>A | $W_b>Q_h$ | $Q_h>Q_h$ | $Q_h>W_b$ | *N* | diol | | dione | |
|---|---|---|---|---|---|---|---|---|
| | B3LYP | B3LYP | B3LYP | | B3LYP | MP2 | B3LYP | MP2 |
| D>A | −5.38(1.99) | −6.30(1.90) | −8.59(1.83) | 2 | −5.87(1.89) | −6.33(1.91) | −12.29(1.72) | −11.24(1.78) |
| D>A>X | −6.17(1.95) | −8.22(1.82) | −9.90(1.79) | 4 | −7.81(1.84) | −8.22(1.87) | −18.65(1.64) | −16.05(1.71) |
| Y>D>A | −7.23(1.86) | −7.20(1.85) | −10.63(1.77) | 6 | −8.89(1.83) | −8.95(1.86) | −21.58(1.59) | −18.22(1.68) |
| Y>D>A>X | −7.16(1.85) | −8.53(1.80) | −10.39(1.75) | 8 | −9.35(1.83) | | −23.99(1.58) | |
| Y>D>A>X>Z | −8.18(1.78) | −9.51(1.73) | −11.89(1.71) | 10 | −9.56(1.82) | | −23.75(1.58) | |
| U>Y>D>A>X | −9.56(1.78) | −9.21(1.78) | −11.41(1.71) | ∞ | −9.83 | −9.41 | −24.34 | −20.00 |

[a] D: proton donor molecule, A: proton acceptor molecule, X,Y,Z,U: additional molecules involving H-bonds ($Q_h$ or $W_b$). The H-bond relay system is given by ···$Q_h>Q_h>W_b>Q_h>Q_h>W_b>Q_h>Q_h>W_b$···. The B3LYP/6-31G* H-bond energies are given with 50% BSSE correction. The asymptotic value for $n = \infty$ is evaluated using the exponential decay plot.

orbital (NBO) charges of H and O atoms involving in the same H-bond, are (0.500, −0.943) au, while in the case of $W_b>Q_h$ the values are (0.489, −0.724). Thus, the charge of O in water is much more negatively charged than that in quinone. Thus, the H-bond in $Q_h>W_b$ is much more ionic than that in $W_b>Q_h$. This explains why the former is shorter and stronger than the latter. Compared with $W_b>Q_h$, the $Q_h>W_b$ has shorter O···H distance (by ∼0.15 Å) and larger binding energy (by ∼3 kcal/mol). This is due to the fact that the lone pair electrons in the water oxygen atom are more stabilized than those in the quinone oxygen atom. This phenomenon is also noted from the water clusters and their hydrated ions.[27]

The differences in H-bond length between the three H-bond types in the dimer formation are well reflected in the calculated NMR chemical shifts ($\delta$: 3.65, 6.78, and 7.24 ppm) (Figure 2). These results would be reliable, since the calculated chemical shifts for the H-bonds of the four-membered ring structure composed of four OH groups in the CHQ monomer ($\delta$: 9.37 ppm for OH) well reproduce our NMR experimental data ($\delta$: 9.83 ppm).

**III. B. H-Bonds Relay.** In Table 2, we report the chain-size effect of the CHQ 1-D H-bond relays, polydiols and polydiones on the H-bond distance. B3LYP/6-31G* results show that the relay effects by the first and second additional H-bonds are important, while those effects by additional H-bonds become less significant. Nevertheless, the H-bond relay seems to have a long-range effect.

In the mid-region of the 9 H-bonds relay system (Figure 4) simulating the X-ray crystal structure of the CHQ tubes, the shortest H···O distances of $W_b>Q_h$, $Q_h>Q_h$, and $Q_h>W_b$ are 1.77, 1.70, and 1.70 Å at the B3LYP/6-31G* level and 1.71, 1.68, and 1.66 Å at the PW-DFT level (Table 3). Both B3LYP/6-31G* and PW-DFT results show that the O···H bond distance in the mid region of the fragment is ∼0.2 Å shorter than those in the terminal region, and ∼0.25 Å shorter than those of the normal H-bonds in the dimer systems ($W_b>Q_h$, $Q_h>Q_h$, or $Q_h>W_b$). At the PW-DFT level, the three distances of the periodic 1-D system or the infinitely long 1-D system decrease down to 1.61, 1.56, and 1.57 Å, respectively. These are slightly

(27) (a) Kim, J.; Suh, S. B.; Kim, K. S. *J. Chem. Phys.* **1999**, *111*, 10077−10087. (b) Kim, J.; Lee, H. M.; Suh, S. B.; Majumdar, D.; Kim, K. S. *J. Chem. Phys.* **2000**, *113*, 5259−5272.

***Table 3.*** H-bond Distances (Å), Enhanced Charges ($\Delta q_H$, $\Delta q_O$; au), and Chemical Shifts ($\delta$, ppm) for Each H-Bond Pair in the H-Bond Relay Systems

| | | $W_b$–$Q_h$ | $Q_h$–$Q_h$ | $Q_h$–$W_b$ | $W_b$–$Q_h$ | $Q_h$–$Q_h$ | $Q_h$–$W_b$ | $W_b$–$Q_h$ | $Q_h$–$Q_h$ | $Q_h$–$W_b$ |
|---|---|---|---|---|---|---|---|---|---|---|
| | | | | | **B3LYP/6-31G*** | | | | | |
| relay (Figure 3) | $d_{O\cdots O}$ | 2.85 | 2.73 | 2.71 | 2.76 | 2.70 | 2.69 | 2.74 | 2.73 | 2.76 |
| | $d_{H\cdots O}$ | 1.91 | 1.75 | 1.71 | 1.79 | 1.70 | 1.70 | 1.77 | 1.75 | 1.77 |
| | $-\Delta q_O$ | 0.047 | 0.073 | 0.054 | 0.067 | 0.079 | 0.054 | 0.069 | 0.068 | 0.014 |
| | $\Delta q_H$ | 0.025 | 0.040 | 0.043 | 0.053 | 0.046 | 0.046 | 0.053 | 0.043 | 0.040 |
| | $\delta$ | 4.7 | 9.0 | 9.6 | 7.2 | 9.9 | 9.9 | 7.4 | 8.9 | 8.3 |
| | | | | | **PW-DFT** | | | | | |
| relay (Figure 3) | $d_{O\cdots O}$ | 2.81 | 2.66 | 2.66 | 2.75 | 2.68 | 2.66 | 2.70 | 2.68 | 2.69 |
| | $d_{H\cdots O}$ | 1.84 | 1.66 | 1.66 | 1.76 | 1.68 | 1.66 | 1.71 | 1.69 | 1.70 |
| | $\delta^a$ | 8.4 | 11.5 | 12.2 | 9.5 | 11.9 | 12.4 | 9.7 | 11.7 | 11.3 |
| infinite-relay with | $d_{O\cdots O}$ | | | | | 2.56 | 2.58 | 2.61 | | |
| no solvent water | $d_{H\cdots O}$ | | | | | 1.56 | 1.57 | 1.61 | | |
| infinite-relay with | $d_{O\cdots O}$ | | | | | 2.56 | 2.51 | 2.72 | | |
| solvent water | $d_{H\cdots O}$ | | | | | 1.56 | 1.51 | 1.72 | | |
| **X-ray structure** | $d_{O\cdots O}$ | | | | | 2.64 | 2.67 | 2.67 | | |

[a] The proton chemical shifts were obtained using B3LYP/6-31G* calculations at the PW-DFT optimized geometry.

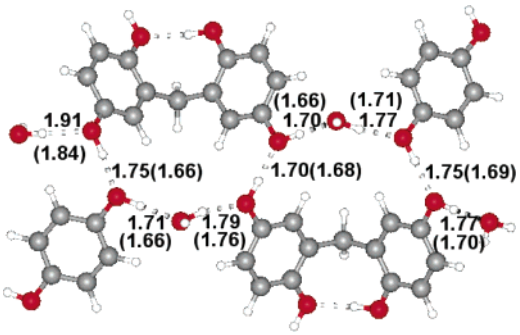


***Figure 4.*** Nine H-bonds relay system showing short H-bonds in a fragment of CHQ nanotube. The H···O bond distances (Å) are given in the figure.

shorter than the corresponding X-ray data (1.67, 1.64, and 1.67 Å in consideration that the H-bond is almost linear and the O−H distance is 1.0 Å). The O···O distances of course show the same trend with the O···H distances because the O···H distances are shorter than the O···O distances by just the OH bond length of 1.0 Å. The three O···O distances by B3LYP/6-31G* (2.74, 2.70, and 2.69 Å in the central region of the 9 H-bonds relay) and PW-DFT (2.70, 2.68, and 2.66 Å in the central region of the 9 H-bonds relay; and 2.61, 2.56, and 2.58 Å for infinitely long relay) are in reasonable agreement with the corresponding X-ray structure (2.67, 2.64, and 2.67 Å). The difference in distance between B3LYP/6-31G* and PW-DFT should not be significantly different because both methods are based on density functionals. Thus, both B3LYP/6-31G* and PW-DFT would predict similar bond distances for infinitely long 1-D H-bonds. It is interesting to note that in the X-ray structure, both $W_b>Q_h$ and $Q_h>W_b$ give the same O···O distances (2.67 Å), while the calculations clearly distinguish the two values (2.74 and 2.69 Å in the 9 H-bonds relay at the B3LYP/6-31G* level; 2.70 and 2.66 Å in the 9 H-bonds relay and 2.61 and 2.58 Å for the infinitely long H-bonds relay at the PW-DFT level). We believe that the same O···O distances for the two cases in the X-ray structure seem to be due to the averaging effect (of the disorder and motion of the H atoms; often noted as half occupancies of OH···O and O···HO). The SHB distances in the 1-D H-bonds relay predicted by PW-DFT are slightly smaller than the X-ray values by ∼0.08 Å. A similar size of deviation of the calculated distances (by B3LYP/6-31G*) from the X-ray data was noted in our previous study of SSHBs in enzymes.[13]

The average H-bond energy and average distance of the normal H-bonds (related to the CHQ system) are ∼6.8 kcal/mol and ∼2.9 Å at the B3LYP/6-31G* level (Table 1). The SHB in the 4 H-bonds relay [∼10.1 kcal/mol, ∼2.75 Å] (Table 2) are ∼3.3 kcal/mol stronger and ∼0.15 Å shorter than the corresponding normal H-bonds. These trends are further enhanced in the SHB of the infinite H-bonds relay (∼2.6 Å) which are ∼0.3 Å shorter than the normal H-bonds. Although the energy strength and bond shortening of the SHB are slightly less than those of SSHBs (>10 kcal/mol, <2.6 Å), the present SHBs have some characteristics of SSHBs or are close to the on-set of the SSHB characteristics. On the basis of the exponential decay plot (where the bond energy in the case of $W_b>Q_h$ is assumed to be smaller than that of $Q_h>W_b$), the asymptotic H-bond energies for $W_b>Q_h$, $Q_h>Q_h$, and $Q_h>W_b$ in the infinite H-bonds relay are estimated to be ∼11, ∼11, and ∼12 kcal/mol, and the average value of these H-bond energies is ∼11.3 kcal/mol with ∼4.5 kcal/mol energy gain over normal H-bond.

As shown in Table 2, the increment in the H-bond energy in the CHQ H-bond relay system does not change smoothly with the increasing number of H-bonds because of distortion of conformations due to the side effects such as those by $\pi-\pi$ interactions, steric repulsions, and additional H-bonds between neighboring aromatic rings. Therefore, to obtain a more accurate H-bond relay effect in the linear system which does not involve other interactions, we have carried out the linear H-bonds relay composed of CHOH═CHOH molecules. From the investigation of B3LYP/6-31G*-predicted H-bond energies from the dimer [$(CHOH═CHOH)_2$] to decamer [$(CHOH═CHOH)_{10}$], we note that the normal H-bond energy is 5.9 ± 0.7 kcal/mol, and the H-bond energies for the tetramer, hexamer, octamer, and decamer are 7.8 ± 0.7, 8.9 ± 0.5, 9.4 ± 0.4, and 9.6 ± 0.3, respectively. Here, the uncertainties reflect ±50% of the BSSE. The asymptotic value is ∼9.8 kcal/mol, and thus the H-bond energy gain of the infinite H-bonds relay over the normal H-bond is ∼3.9 kcal/mol. This result is consistent with that in the CHQ system.

Since the binding energy gain due to the SHB (∼3.9 kcal/mol) is large, we investigated the atomic charges of H and O atoms involving the donor−acceptor H···O bond pair in the dimers and the 9 H-bonds relay, based on the natural bond orbital population analysis at the B3LYP/6-31G* level (Figures

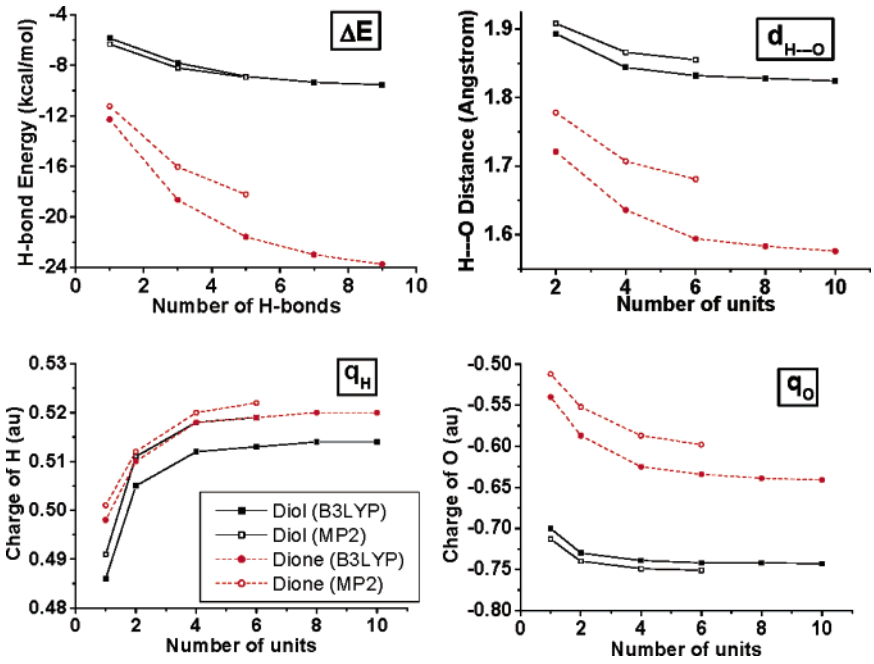


***Figure 5.*** H-bond interaction energies ($\Delta E$), H···O H-bond distances ($d_{H\cdots O}$), and NBO atomic charges of H and O atoms ($q_H$, $q_O$) for the central H-bond in the linear chainlike *n*-polymers of 1,2-ethanediols and 1,3-propanediones.

3 and 4). The charges of H and O ($q_H$, $q_O$) in the non-H-bonded isolated systems of $W_b$ and $Q_h$ are (0.466, −0.933) and (0.483, −0.695) au, respectively. In the H-bonded dimers of $W_b > Q_h$, $Q_h > Q_h$, and $Q_h > W_b$ (Figure 3), the atomic charges ($q_H$, $q_O$) in the H···O pair are (0.489, −0.723), (0.506, −0.728), and (0.500, −0.943) au. The case of $Q_h > W_b$ has much stronger electrostatic interaction than the case of $W_b > Q_h$, which reflects the stronger binding energy of the former. In the 9 H-bonds relay, the most enhanced charges ($\Delta q_H$, $\Delta q_O$) for the cases of $W_b > Q_h$, $Q_h > Q_h$, and $Q_h > W_b$ (associated with the shortest H-bond lengths in the central region) [(0.053, −0.069), (0.046, −0.079), and (0.046, −0.054) au, respectively] are much larger than those in the terminal region and those in the corresponding dimer systems [(0.022, −0.028), (0.028, −0.033), and (0.013, −0.010) au, respectively]. Thus, the large energy gain in SHB arises from the strong polarization effect along the H-bonds relay chain. It is also correlated to the H-bond length (Figure 4) and NMR chemical shifts. In this case, the charge dissipation effect should not be significant because of the absence of the anionic site such as oxyanion in enzymes wherein the charge dissipation effect is important.[13] Shorter H-bonds show large chemical shifts (up to 12.44 ppm for $Q_h > W_b$ in the central region of the 9 H-bonds relay at the PW-DFT geometry similar to the X-ray geometry). The chemical shift for the infinitely long 1-D H-bonds relay (which should be larger than 12.4 ppm at the O···O H-bond distance of 2.66 Å) is much larger than the chemical shift for the four-membered circular H-bonds (9.37 ppm) in the CHQ monomer as well as those of the dimers. In this regard, it would be intriguing to investigate the proton tunneling in the infinitely long 1-D H-bonds relay, as the proton tunneling in the four-membered circular H-bonds in calix[4]-arene systems has been investigated.[28] It is also interesting to note that the $Q_h > W_b$ H-bonds show larger chemical shifts and shorter H-bond lengths than the $W_b > Q_h$, as the former has stronger H-bond strength.

Since we have investigated the H-bond relay effect in the CHQ nanotube, it would useful to compare this CHQ SHB with the H-bonds of the linear chainlike diol and dione H-bond arrays on a plane. Here, the H-bond relay effects of 1,2-ethanediol and 1,3-propanedione have been investigated up to the decamer at the B3LYP level and up to the hexamer at the MP2 level (refer to the interaction energies, bond distances, and atomic charges in Figure 5). Interaction energies of the diol dimer and the dione dimer are −5.87 and −12.29 kcal/mol for B3LYP, respectively, and −6.33 and −11.23 kcal/mol for MP2, respectively. The asymptotic values are −9.8 and −24.2 kcal/mol at the B3LYP level, and −9.4 and −20.0 kcal/mol at the MP2 level. As the number of H-bonds increase, the NBO atomic charges as well as H-bonding energies increase, and H-bond distances decrease.

**III. C. Infinitely Long 1-D SHB and the Solvent Effect.** The binding energy corresponds to the energy to dissociate one H-bond in the long H-bonds relay chain. This energy is correlated to the average energy gain per SHB (i.e., $-E_{shb}$). To obtain this latter quantity as well as the changes in H-bond distance in the infinite chain of the CHQ crystal, we carried out PW-DFT calculations of the CHQ tubes array system using the crystal structure. In addition, we investigated the binding energy gain/loss of SHB due to the solvation effect in the explicit presence of solvent molecules.

We denote $Q_c$, $W_b$, and $S_w$ as a CHQ monomer, a water molecule bridging two adjacent CHQ monomers in the CHQ tube, and a solvent water molecule, respectively. Each unit cell has $n_q$ $Q_c$'s, $n_w$ $W_b$'s, and $n_s$ $S_w$'s where $n_q = 4$, $n_w = 8$, and $n_s = 24$. The number of solvent water molecules (excluding the bridging water molecules) per unit cell in the CHQ tubes, $n_s$, was determined from the water accessible volume. We consider

(28) Brougham, D. F.; Caciuffo, R.; Horsewill, A. J. *Nature* **1999**, 397, 241−243.

***Table 4.*** Energy Analysis (in eV) of the System without Solvent (A) and the System with Solvent (B)

| system(A) | | system (B)[h−n] | |
|---|---|---|---|
| $n_q$, $n_w$, $n_s$ | 4, 8, 0 | $n_q$, $n_w$, $n_s$ | 4, 8, 24 |
| $E_A(Q_c's,W_b's)$[a] | −1704.369 | $E_B(Q_c's,W_b's,S_w's)$[e] | −2059.532 |
| $E_A(Q_c's)$[b] | −1583.459 | $E_B(Q_c's,W_b's)$[f] | −1703.317 |
| $E_A(W_b's)$[c] | −113.397 | $E_B(S_w's)$ | −349.078 |
| $\Delta E_A^{hb}(Q_c{-}W_b's)$[d] | −4.071 | $E_B(W_b's,S_w's)$[g] | −466.639 |
| $\Delta E_A^{shb}(-Q_c{-}W_b{-}Q_c{-}'s)$ | −3.442 | $\Delta E^{solv}(-W_b{-}Q_c{-}Q_c{-}'s)$ | 1.052 |
| ($\Delta E_A^{shb}$ per SHB) | −3.442/24 | $\Delta E^{solv}$ per SHB | 1.052/24 |
| | (−3.9kcal/mol) | ($\Delta E_B^{shb}$ per SHB) | (1.2kcal/mol) |
| | | | (−2.7kcal/mol) |

[a] $E_A(Q_c's,W_b's) = E_A(Q_c's) + E_A(W_b's) + E_A^{hb}(Q_c{-}W_b's) + E_A^{shb}(-Q_c{-}W_b{-}Q_c{-}'s)$. [b] $E_A(Q_c's) \approx n_q\, E_1(Q_c) + n_q\, E_1^{hb}(Q_c{-}Q_c's) + E_A^{\pi}(Q_c{:}Q_c's)$. [c] $E_A(W_b's) \approx n_w\, E_1(W_b)$. [d] $E_A^{hb}(Q_c{-}W_b's) \approx n_w\{E_A^{hb}(Q_c{>}W_b) + E_A^{hb}(W_b{>}Q_c)\}$. [e] $E_B(Q_c's,W_b's,S_w's) = E_B(Q_c's,W_b's) + E_B(W_b's,S_w's) - E_B(W_b's) + \{E_B(Q_c's,S_w's) - E_B(Q_c's) - E_B(S_w's)\}$. [f] $E_B(Q_c's,W_b's) = E_A(Q_c's,W_b's) + E_{solv}(-W_b{-}Q_c{-}Q_c{-}'s)$. [g] $E_B(W_b's,S_w's) = E_B(W_b's) + E_B(S_w's) + E_B^{hb}(W_b's,S_w's)$. [h] $E_B(Q_c's,S_w's) = E_B(Q_c's) + E_B(S_w's) + E_B^{hb}(Q_c's,S_w's)$. [i] $E(W_b's,W_b's) \approx 0$. [j] $E_B(Q_c's) \approx E_A(Q_c's)$. [k] $E_B(W_b's) \approx E_A(W_b's)$. [l] $E_B(S_w's) = n_s\, E_1(S_w) + E_B^{hb}(S_w's, S_w's)$. [m] Deformation energies of Q and W are almost neglected. [n] $E_1$ denotes the energy of a single molecule.

two different systems: (A) a system without solvent water molecules and (B) a system including solvent water molecules.

Then, the total energy of system (A) per unit cell is $E(Q_c's,W_b's) = E(Q_c's) + E(W_b's) + \Delta E_{hb}(Q_c{-}W_b's) + \Delta E_{shb}(-Q_c{-}W_b{-}Q_c{-}'s)$, where subscripts "hb" and "shb" denote H-bonding and SHB, respectively. As shown in the partitioning scheme of the interaction energy components in Table 4, we obtain $E_{shb}$/SHB = −3.9 kcal/mol. Thus, the average energy gain by one SHB over one normal H-bond is estimated to be 3.9 kcal/mol. Considering that the average H-bond energy per normal H-bond in the CHQ tubes is 6.2 kcal/mol at the PW-DFT level, the average H-bond energy per SHB in the CHQ tube is 10.1 kcal/mol, which is comparable to the bond dissociation energy (∼11 kcal/mol) of one SHB in the linear chain.

To obtain the solvent effect, the structure of system (B) was also optimized. Here, we briefly discuss the analysis of hydration structure in the CHQ tubes. A half unit cell corresponding to a single nanotube has 4 CHQs with 8 $W_b$'s. In this case, the number of water molecules in the first, second, and third hydration shells are 8, 12, and 4, respectively. The structure of CHQs in water is found to be almost identical to that without solvent water, and thus, it is of course similar to the X-ray structure. The water molecules in the first hydration shell seem to be bound to either bridging water molecules or the OH groups in $Q_h$ moieties in CHQ. The water molecules in the second hydration shell are mobile at room temperature, and those in the third hydration shell are randomized. Figure 6 shows the energy-minimized structure of the water molecules in the nanotube which can be considered as one of the most significant conformations. If the water molecules are fully dried up, a half unit cell should have only 8 $W_b$'s. When it is fully solvated, it has about 24 solvent water molecules ($S_w$'s), which correspond to the volume ∼720 Å$^3$, or cross section of 8 × 8 × 11.2 Å$^3$.

From the results of (A) and (B), it is interesting to note that the H-bond distances are only slightly changed. The O···O distances of $W_b{>}Q_h$, $Q_h{>}Q_h$, and $Q_h{>}W_b$ in system (A) at the PW-DFT level are 2.61, 2.56, and 2.58 Å, respectively, while those in system (B) are 2.72, 2.56, and 2.51 Å, respectively (Table 3). Thus, the O···O distances for $Q_h{>}Q_h$ (2.56 Å) hardly change by solvent water because water molecules do not exist near the H-bond interaction sites of $Q_h{>}Q_h$. On the other hand, the O···O distance of $W_b{>}Q_h$ is lengthened by 0.11 Å, whereas that of $Q_h{>}W_b$ is shortened by 0.07 Å due to the solvent effect. The overall average O···O distance for the above three cases is lengthened by only 0.01 Å, which is insignificant, but shows

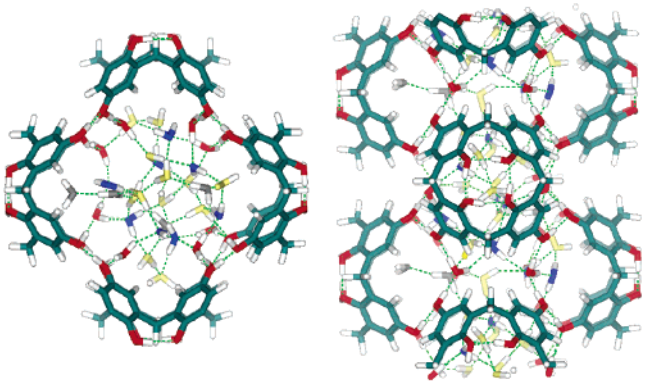

***Figure 6.*** Water network in a single tube (top and side views). The top view (left) shows 8 bridging water molecules in red, 8 first-hydration shell water molecules in blue, 12 second-hydration shell water molecules in yellow, and 4 third-hydration-shell water molecules in gray, while the side view shows twice those in the top view.

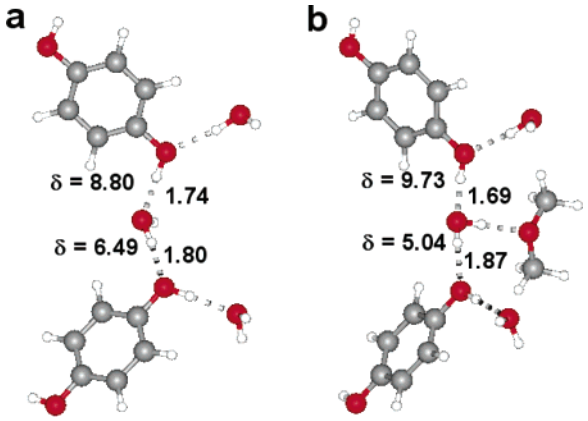


***Figure 7.*** Changes in H-bond distances of system $W_b{-}Q_h{-}W_b{-}Q_h{-}W_b$ by adding a solvent water molecule H-bonded to the central bridging water molecule (B3LYP/6-31G* calculations). The H-bond distances for $Q_h{>}W_b$ and $W_b{>}Q_h$ in (a) are 1.74 and 1.80 Å, respectively, while those in (b) are 1.69 and 1.87 Å, respectively.

slight weakening of the short H-bond strength. This weakening is related to the anti-catalytic effect on enzymes by polar solvents. The structural change by the solvent can be evidenced from the structural change by an additional solvent molecule (acetone) of a system shown in Figure 7. By adding an acetone molecule, the H-bond distance for $W_b{>}Q_h$ increases by 0.07 Å, whereas that for $Q_h{>}W_b$ decreases by 0.05 Å; the presence of one additional acetone molecule increases the average H-bond distance only by 0.01 Å. Thus, the existence of one nearby acetone molecule explains two-thirds of the solvent effect in

this system. The effect by a water molecule (which is considered to be almost the same as that by an acetone molecule) was not studied because of the presence of unwanted extra interactions in a small CHQ fragment by the water H atoms with other neighboring bridging-water molecules in the chain.

The energy of the optimized system (B) [$E(Q_c\text{'s},W_b\text{'s})$] is higher than the energy of system (A) by 1.052 eV due to the solvent contribution ($E_{sol}$). The solvent contribution per SHB (24 HBs total) is 1.2 kcal/mol (Table 4), which weakens the H-bond strength. Thus, the average HB energy per SHB in the presence of solvent water molecules is 8.9 kcal/mol which is 2.7 kcal/mol larger than the average normal H-bond energy. Although our calculation approach is not very accurate, the quantity should be reasonably reliable.

## IV. Concluding Remarks

As already discussed, the enhanced bond dissociation energy in a SHB in an infinitely long chain is ∼4 kcal/mol, and the highly enhanced binding energy per SHB in the CHQ crystal in the absence of solvents is 3.9 kcal/mol. However, in the presence of solvent water molecules, the strength of SHB in the CHQ crystal is slightly decreased, but it has still significantly enhanced binding energy per SHB (by 2.7 kcal/mol). The anti-catalytic effect by the solvent is small (i.e., only by ∼1 kcal/mol). In the cases of double H-bonded systems or partly double H-bonded systems, both normal H-bond and SHB energies (∼11 and ∼20 kcal/mol, respectively) increase twice as much as those of the single H-bond systems (∼6 and ∼10 kcal/mol, respectively).

**Acknowledgment.** This contribution is dedicated to Prof. Dong Han Kim on the occasion of his 70th birthday. This work was supported by creative Research Initiative of Korea Institute of Science and Technology Evaluation and Planning. Most of the calculations were carried out using supercomputers (NEC-SX6, IBM/SP2, and Compac/Dec Workstation Clusters) in KORDIC.

JA037607A